

# Machinability Analysis of Heat Treated Ti64, Ti54M and Ti10.2.3 Titanium Alloys

Navneet Khanna<sup>1,#</sup> and Kuldip Singh Sangwan<sup>1</sup>

<sup>1</sup> Mechanical Engineering Department, BITS Pilani, Pilani, Jhunjhunu, Rajasthan, India, 333-031  
# Corresponding Author / E-mail: khannanavneet@gmail.com, TEL: +91-97-850-11178, FAX: +91-1596-244183

KEYWORDS: Cutting force, Friction coefficient, Heat treatment, Machinability, Temperature, Titanium alloys

*In this research, machinability of the heat treated  $\alpha/\beta$  (Ti64 and Ti54M) and metastable  $\beta$  (Ti10.2.3) titanium alloys is investigated experimentally. Forces and temperature i.e. life of the cutting tool mainly influenced by variation in cutting speed and feed rate, therefore, the depth of cut was maintained constant while cutting speed and feed were varied. Heat treatment was found to have influence on the machinability of the analyzed alloys. The annealed and solution treated plus over aged samples of the Ti10.2.3 alloy, showed comparatively higher cutting tool temperature and higher cutting forces. This work confirmed the poorer machinability of the Ti10.2.3 alloy than the Ti64 and Ti54M alloys in different heat treatment conditions and this is due to the presence of higher content of  $\beta$  stabilizer elements (V and Fe). It is concluded that the proper heat treatment planning results in better machining performance of the titanium alloys.*

Manuscript received: October 15, 2012 / Accepted: March 5, 2013

## NOMENCLATURE

$\alpha$  = alpha  
 $\beta$  = beta  
 STOA = solution treated plus over aged  
 HRC = rockwellC hardness  
 $K_c$  = specific cutting force  
 $K_f$  = specific feed force  
 $\mu$  = friction coefficient  
 $F_{Chvc}$  = chip forming cutting force  
 $F_{Chvf}$  = chip forming feed force  
 $r_\epsilon$  = corner radius  
 $r_\beta$  = cutting edge roundness  
 $\gamma_0$  = rake angle  
 $\kappa_r$  = cutting edge angle  
 $\lambda_s$  = cutting edge inclination angle  
 $V_c$  = cutting speed  
 $f$  = feed rate  
 $a_p$  = depth of cut

machinability of titanium and its alloys has been become an important topic of investigation nowadays. Titanium alloys have low thermal conductivity; which subsequently increases the temperature at the edge of the cutting tool. Hence, leads to the accumulation of high amounts of heat and mechanical stress around the cutting tool edge at high feed rates and cutting speeds, consequently increasing the cutting temperature and cutting forces which leads to catastrophic tool failure.<sup>1</sup> Additionally, it's low young's modulus, high chemical reactivity with many cutting tool materials and high strength at elevated temperature further impair its machinability.<sup>2</sup>

Lightweight aero-structural components are often made of the well-established Ti64 titanium alloy, which belongs to the  $\alpha/\beta$  family of the titanium alloys and represents more than 50% of the worldwide titanium production.<sup>3</sup> Ti54M is also an  $\alpha/\beta$  titanium alloy which provides cost benefits with superior machinability and strength comparable to similarly processed Ti64.<sup>4-7</sup> Ti10.2.3 is the structural  $\beta$  titanium alloy and is of increasing interest for prospective applications such as landing gears, rotor heads and fasteners.<sup>8,9</sup> Several works have been published concerning the machining of commonly used alloy Ti64. However, limited machining data is encountered for titanium alloys Ti54M<sup>7</sup> and Ti10.2.3.<sup>6,8</sup>

In order to analyze the effect of heat treatment, comparison of the machinability of the newly developed Ti54M alloy and increasingly

## 1. Introduction

Titanium alloys are very difficult to machine materials. The

Table 1 Chemical composition and mechanical properties of the Ti64, Ti54M and Ti10.2.3 alloys

Titanium Alloy	Chemical Composition (%)				Transus $\beta$ (°C)	Al Equiv. Value (wt. %)	Mo Equiv. Value (wt. %)	TYS (MPa)	UTS (MPa)	Elongation (%)
	Al	Mo	V	Fe						
Ti64	6	-	4	0.15	995	6	3.1	910	990	18
Ti54M	5	0.8	4	0.5	966	5	5	860	935	23
Ti10.2.3	3	-	10	2	800	3	12	1100	1200	9

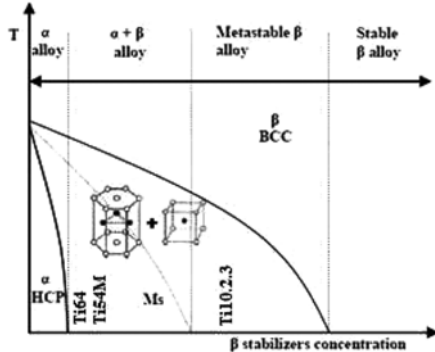
Fig. 1 Titanium phase stability as a function of concentration of temperature and  $\beta$  stabilizers

Table 2 Heat treatment conditions and hardness for the analyzed titanium alloys

Titanium Alloy	Heat Treatment	Hardness (HRC $\pm$ 3)
Ti64	Annealed 750°C	31
Ti54M	Annealed 705°C	31
Ti54M	$\beta$ annealed (990°C (1 h) - water quench)	35
Ti10.2.3	Annealed 760°C	32
Ti10.2.3	STOA (750°C (2 h) -air cool + 565°C (8 h)- air cool)	32

used  $\beta$  alloy Ti10.2.3 in two different heat treated conditions vis-à-vis the extensively used Ti64 alloy is presented. Firstly, the experimental plan and set up including the details of the investigated titanium alloys are presented, after that, results are discussed and finally, overall conclusions are highlighted.

## 2. Experimental Plan and Setup

### 2.1 Workpiece Materials

Chemical composition and mechanical properties of all the titanium alloys are summarized in Table 1.

It is observed that the Ti10.2.3 alloy present a molybdenum equivalent value, roughly 4 and 2.5 times higher than the Ti64 and Ti54M; respectively. This value explains the higher mechanical properties of this metastable  $\beta$  titanium alloy as compared to  $\alpha/\beta$  titanium alloys. Due to the presence of higher concentration of  $\beta$  stabilizers (Fe and V), in Ti10.2.3 alloy, the  $\beta$  transus temperature is almost 195°C and 166°C lower than that of Ti64 and newly developed Ti54M alloys (Fig. 1); respectively. The details of the performed heat treatments are summarized in Table 2.

### 2.2 Machining Arrangement

Orthogonal machining tests were carried out in Lagun CNC



Fig. 2 Experimental setup

Table 3 Cutting conditions

$V_c$ (m/min)	40; 80
$f$ (mm/rev)	0.1; 0.15; 0.25
$a_p$ (mm)	2
Coolant	Dry (No coolant)

machining centre (Fig. 2) using titanium hollow tubes of 48 mm diameter and 2 mm thickness as workpieces. For eliminating material heterogeneities produced in forged specimens, a material thickness varying from 5 to 10 mm was eliminated from outside diameter.

The tool inserts were clamped on a tool holder of specification DCLNR 2525 M12. Tool inserts conform the specification TNMG 120408-23. This combination of tool holder and tool insert provides the following tool geometry features:

$$\begin{aligned} r_e &= 0.8 \text{ mm} \\ r_\beta &= 34 \pm 2 \text{ } \mu\text{m} \\ \gamma_0 &= 7^\circ \\ \kappa_r &= 0^\circ \\ \lambda_s &= 0^\circ \end{aligned}$$

Tests were repeated at least twice in all cases with the purpose of estimating uncertainty.

A micro thermal imaging system consisting of a FLIR Titanium 550 M infrared camera and a microscopic lens offering a 10  $\mu\text{m}$  resolution were used to measure temperatures on the cutting edge during the machining of all alloys. The cutting conditions used in the trials are shown in Table 3.

## 3. Results and Discussion

An analysis of variance (ANOVA) was conducted to identify statistically significant trends in the measured data for cutting and feed forces as well as cutting tool temperature with respect to the different heat treatment conditions and cutting parameters.

Table 4 ANOVA for  $K_c$  at 40 m/min

Source	DF	MS	F	P-value	
Heat Treatment	4	74357.62	265.337	0.000	Significant
Feed Rate	2	726679.6	2593.075	0.000	Significant
Interaction	8	5002.918	17.852	0.000	Significant
Error	30	280.2386			
Total	44				

Table 5 ANOVA for  $K_c$  at 80 m/min

Source	DF	MS	F	P-value	
Heat Treatment	4	7256.207	18.659	0.000	Significant
Feed Rate	2	854716.7	2197.925	0.000	Significant
Interaction	8	2501.568	6.433	0.000	Significant
Error	30	388.875			
Total	44				

Table 6 ANOVA for  $K_k$  at 40 m/min

Source	DF	MS	F	P-value	
Heat Treatment	4	126484.8	93.339	0.000	Significant
Feed Rate	2	2646655	1953.095	0.000	Significant
Interaction	8	10347.75	7.636	0.000	Significant
Error	30	1355.109			
Total	44				

Table 7 ANOVA for  $K_k$  at 80 m/min

Source	DF	MS	F	P-value	
Heat Treatment	4	12391.51	7.796	0.000	Significant
Feed Rate	2	2334302	1468.536	0.000	Significant
Interaction	8	2409.443	1.5158	0.193	Not Significant
Error	30	1589.544			
Total	44				

Table 8 ANOVA for cutting tool temperature at 40 m/min

Source	DF	MS	F	P-value	
Heat Treatment	4	33871.3	300.989	0.000	Significant
Feed Rate	2	192557.2	1711.112	0.000	Significant
Interaction	8	1942.767	17.264	0.000	Significant
Error	30	112.533			
Total	44				

Table 9 ANOVA for cutting tool temperature at 80 m/min

Source	DF	MS	F	P-value	
Heat Treatment	4	25081.3	60.212	0.000	Significant
Feed Rate	2	152512.4	366.127	0.000	Significant
Interaction	8	2479.217	5.952	0.000	Significant
Error	30	416.556			
Total	44				

### 3.1 ANOVA Results

ANOVA tables for  $K_c$ ,  $K_k$  and cutting tool temperature parameters for different heat treated titanium alloys are given in Tables 4-9. In addition to degree of freedom (DF), mean square (MS) and F-values (F) the table shows the P-values (P) associate with each input factor and their interaction. A low P-value indicates statistical significance for the source on the corresponding response.<sup>10,11</sup> Tables 4-9 show that the main effects of heat treatment along with varying chemical

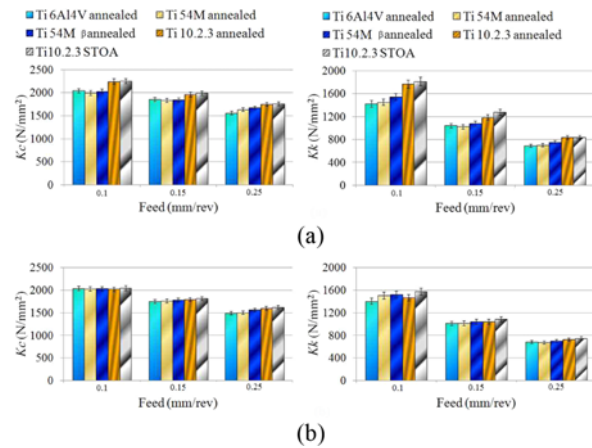


Fig. 3 Specific cutting and feed forces at cutting speed of (a) 40 m/min and of (b) 80 m/min

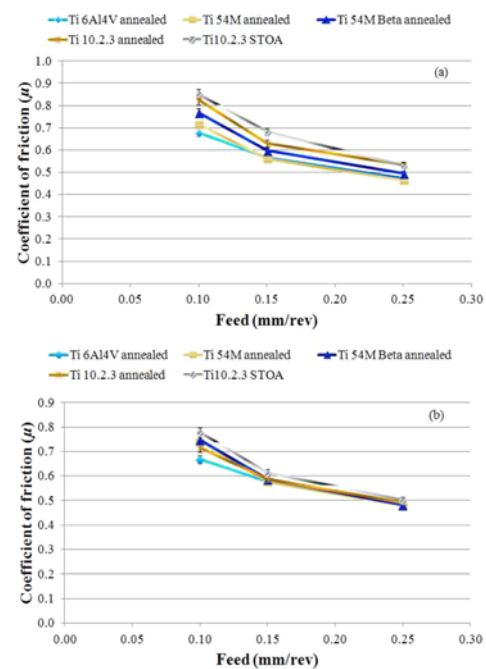


Fig. 4 Friction coefficient at cutting speed of (a) 40 m/min and of (b) 80 m/min

composition, feed rate and also interactions between them are statistically significant to  $K_c$ ,  $K_k$  and cutting tool temperature for all the experiments, except at  $V_c = 80$  m/min, where interaction is found to be statistically insignificant. Heat treatment along with varying chemical composition are the dominant parameters associated with the  $K_c$ ,  $K_k$  and cutting tool temperature.<sup>5,6</sup> This is expected because it is well known that the microstructural changes due to heat treatment and chemical composition have influence on the machinability of the titanium alloys.<sup>8,9</sup>

### 3.2 Specific Cutting and Feed Forces

The cutting forces during experimental trials were measured by a 3-component dynamometer (Kistler 9121). The specific cutting and specific feed forces for all the analyzed titanium alloys at two cutting speeds (40 and 80 m/min) are shown in Fig. 3(a) and (b), respectively.

Results plotted for the specific forces represent the mean values

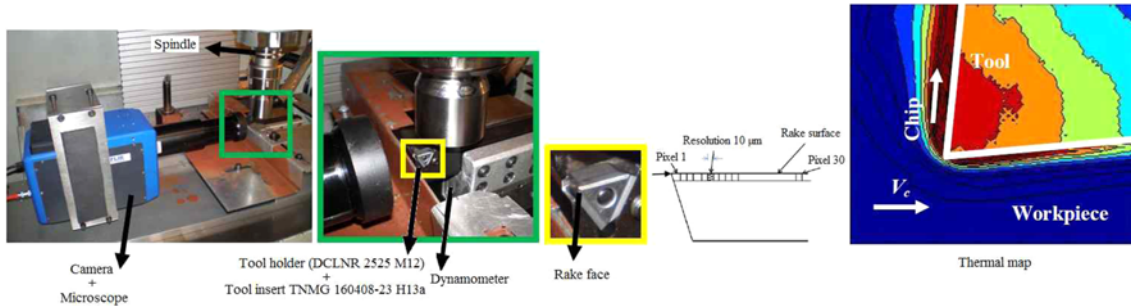


Fig. 5 Temperature measuring details

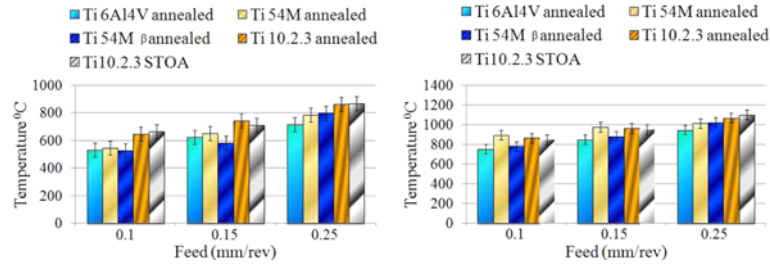


Fig. 6 Temperature at cutting speed of (a) 40 m/min and of (b) 80 m/min



Fig. 7 Temperature measurement steps

observed from the experimental tests. In machining the titanium alloys the results presented in Fig. 3(a) and Fig. 3(b) show that the specific cutting force decreases with the increase in feed rate. This trend is followed in all heat treatment conditions. The highest specific cutting forces were noticed for Ti10.2.3 STOA at all cutting parameters. The lower specific cutting forces were observed for Ti54M annealed at all feed rates ( $V_c = 40$  m/min). The higher specific cutting force achieved while machining Ti10.2.3 in STOA condition is due the formation of secondary  $\alpha$  precipitates in the  $\beta$  matrix. This microstructure seems to produce higher shear stress and in consequence higher cutting force.

Variation in the specific feed force follows the same trend and decreases rapidly with the increase of feed rate and gets almost halved on increasing the feed value from 0.1 to 0.25 mm/rev. At cutting speed of 40 m/min; the highest specific feed forces were observed for Ti10.2.3 STOA followed by Ti10.2.3 alloy in annealed condition. Same trend was observed at cutting speed of 80 m/min except at feed rate of 0.1 mm/rev. The specific feed force values correlated well with the mechanical properties of the alloys, as higher values were obtained for the Ti10.2.3 alloy. High strength of Ti10.2.3 is the reason for its higher specific feed forces and this high strength is resulting from the precipitation of  $\alpha$  during the aging process carried out after solution treatment.

Thus, the differences between the  $\alpha/\beta$  and the metastable  $\beta$  titanium alloys in different heat treated conditions are comparatively more apparent in the case of the specific feed force than in the specific cutting force.

### 3.3 Friction Coefficient Analysis

Wyen and Wegener<sup>12</sup> reported that the friction coefficient is influenced by both the cutting speed and cutting edge radius while

cutting Ti64 titanium alloy. Khanna and Sangwan<sup>6,7</sup> showed dependence of the friction coefficient on feed rate and heat treatment conditions during machining Ti54M and Ti10.2.3 titanium alloy. The average coefficient of friction is calculated by using following equation (1); used by Wyen and Wegener<sup>12</sup>

$$\mu = (F_{ch,c} \sin \gamma_0 + F_{ch,r} \cos \gamma_0) / (F_{ch,c} \cos \gamma_0 - F_{ch,r} \sin \gamma_0) \quad (1)$$

Fig. 4(a) and (b) shows that the coefficient of friction versus feed rate for both  $\alpha/\beta$  and metastable  $\beta$  titanium alloys in different heat treatment condition. For all feed rates at cutting speed of 40 m/min, the data consistently show that the  $\mu$  is in the order of high to low as: Ti10.2.3 STOA > Ti10.2.3 annealed > Ti54M  $\beta$  annealed > Ti64 annealed > Ti54M annealed; except at feed rate of 0.1 mm/rev where Ti54M shows more value of  $\mu$  than Ti64. The coefficient of friction was found to be decreased with the increase of feed rate even though the temperature increases during machining all the titanium alloys. This drop in the friction coefficient is due to the chip's hot softening and consequent reduction in the chip's resistance to sliding with the tool rake surface.<sup>6,7</sup> The larger decrease in friction coefficient was observed when the feed rate changes from 0.1 to 1.5 mm/rev in comparison to the change in feed rate from 0.15 to 0.25 mm/rev for both the cutting speeds.

### 3.4 Cutting Tool Temperature

Thermal radiation in the narrow range of 3.97-4.01  $\mu\text{m}$  was measured by a microscope consisting of a 320 by 256 cooled indium antimonide focal plane array and a germanium lens. The imaging system is capable of acquiring 40 Mpixels/s. The integration time was fixed at 200  $\mu\text{s}$ .

The detector was calibrated against a black body with controlled temperature and an emissivity independent of the wavelength. The emissivity of the workpiece and tool materials as a function of wavelength and temperature were measured with a Fourier transform infrared spectrometer.<sup>4</sup> The narrow band of accepted radiation obviated the wavelength variation and, thus, only the influence of temperature was taken into account: a different value of emissivity was applied to each pixel depending on its blackbody temperature. In the wavelength range, the average value of emissivity was 0.3 for the tailored carbide tool.<sup>5</sup> The thermal measuring system was focused on the tool/chip interface (Fig. 5), thus making dynamic thermal measurement acquisitions possible.

The influence of cutting parameters along with heat treatment conditions on the local tool temperature is shown in Fig. 6 (a) and Fig. 6(b). Although the temperature has been measured during complete machining process of 5 sec duration, the temperature values were extracted for the last 1 sec of cut because; it is closer to a stationary behavior. These values are the mean of three readings for each cutting condition. All the step-wise details of temperature measurement are presented in Fig. 7.

The local tool temperature values of both the Ti10.2.3 alloys; which have relatively higher strength values are higher than  $\alpha/\beta$  alloys; especially at cutting speed of 40 m/min (Fig. 6(a)). The specific feed force shows the quantity of friction and rubbing effects over the rake surface and thus, the amount of heat generated at the tool/chip contact zone.<sup>3</sup> Therefore, high tool wear are expected in the Ti10.2.3 alloys as compared with  $\alpha/\beta$  titanium alloys.

An unclear difference in local tool temperature is observed at cutting speed of 80 m/min (Fig. 6(b)). This distinction does not coincide well with an identifiable difference in the specific feed forces (Fig. 3(b)) and apparent coefficient of friction (Fig. 4(b)). However, this might be due to the uncertainty ( $\pm 50^\circ\text{C}^5$ ) in thermal measurement method. Young's modulus of the titanium alloys decreases with the increase in temperature of the titanium alloy workpiece.<sup>2</sup> Fluctuations in the tool/chip interface during machining due to this reduction in elastic modulus may be a probable cause of this uncertainty in the thermal measurement system.

No information regarding machining Ti10.2.3 in STOA heat treatment condition is available to the best of our knowledge. It is, therefore; essential to investigate the machinability of this class of alloys in different thermal conditions; so as to reach at a concrete conclusion.

#### 4. Conclusions

From the observed effects of heat treatment on the machining performance of titanium alloys, the following can be concluded.

- There is a close relationship between the machinability rate and the mechanical properties of the work material, chemical composition (Mo equivalent value) as well as the tool temperature, friction coefficient, specific cutting and feed forces.
- Measurement of apparent coefficient of friction over the rake face has revealed the poor machinability of the Ti10.2.3 alloy.
- Temperature generated for Ti10.2.3 STOA alloy is highest at high

cutting parameters. Abrasive effect of the secondary  $\alpha$  precipitates is one of the reasons behind this high temperature.<sup>8</sup>

- Better machinability of Ti10.2.3 is observed in STOA condition than the recent research reported for Ti10.2.3 in solution treated and aged condition (STA)<sup>6</sup> and this is due to the over aging heat treatment. Over aging decreases the hardness of the Ti10.2.3 alloy. This might be due to coalescence of the precipitates into bigger particles which will cause fewer impediments to the movement of dislocation and hence the hardness begins to decrease.
- There is a significant influence of the metallurgical state on the machinability after the forging process and the modification of the thermal treatment in planned way can improve the machinability of the titanium alloys.

#### ACKNOWLEDGEMENT

The present research was carried out within the collaboration of BITS Pilani (India) and MGEP (Spain) to facilitate Mr. Navneet Khanna to undergo training within the Research Group of University of Mondragon-Faculty of Engineering (MGEP) and authors are thankful to them. The authors are extremely grateful to Prof. P. J. Arrazola for providing training in titanium machining at the High-Performance Machining laboratory, Mondragon University, Spain. Authors also acknowledge the support of Dr. Ainhara Garay, Dr. Daniel Soler and Mr. Luis M. Iriarte in completing this research.

#### REFERENCES

1. Rahman Rashid, R. A., Sun, S., Wang, W., and Dargusch, M. S., "An investigation of cutting forces and cutting temperatures during laser-assisted machining of the Ti-6Cr-5Mo-5V-4Al beta titanium alloy," *Int. J. Mach Tools Manuf.*, Vol. 63, No. 11, pp. 58-69, 2012.
2. Komanduri, R. and Hou, Z., "On the thermoplastic shear instability in the machining of a titanium alloy (Ti-6Al-4V)," *Metall. and Mater. Transac.*, Vol. 33A, pp. 2995-3010, 2002.
3. Arrazola, P. J., Garay, A., Iriarte, L. M., Armendia, M., Marya, S., and Maitre, F., "Machinability of titanium alloys (Ti6Al4V and Ti555.3)," *Int. J. Mater. Proc. Technol.*, Vol. 209, pp. 2223-2230, 2009.
4. Armendia, M., Garay, A., Villar, A., Davies, M. A., and Arrazola, P. J., "High bandwidth temperature measurement in interrupted cutting of difficult to machine materials," *CIRP Annals-Manuf. Technol.*, Vol. 59, No.1, pp. 97-100, 2010.
5. Khanna, N., Garay, A., Iriarte, L. M., Daniel, S., Sangwan, K. S., and Arrazola, P. J., "Effect of heat treatment conditions on the machinability of Ti64 and Ti54M alloys," *Procedia CIRP*, Vol. 1, pp. 477-482, 2012.
6. Khanna, N. and Sangwan, K. S., "Machinability study of  $\alpha/\beta$  and  $\beta$  titanium alloys in different heat treatment conditions," *Proc. IMechE. Part B - J. Engng. Manufact.*, Vol. 227, No. 3, pp. 357-361, 2013.

7. Khanna, N. and Sangwan, K. S., "Comparative machinability study on Ti54M titanium alloy in different heat treatment conditions," Proc. IMechE. Part B - J. Engng.Manufact.,Vol. 227, No. 1, pp. 96-101, 2013.
8. Machai, C. and Biermann, D., "Machining of a Hollow Shaft Made of  $\beta$ - Titanium Ti-10V-2Fe-3Al," IEEE International Symposium on Assembly and Manufacturing, pp. 1-6, 2011.
9. Boyer, R. R. and Briggs, R. D., "The Use of  $\beta$  Titanium Alloys in the Aerospace Industry," Journal of Materials Engineering and Performance, Vol. 14, pp. 681-685, 2005.
10. Ramanujam, R., Muthukrishnan, N., and Raju, R., "Optimization of cutting parameters for turning Al-SiC(10p) MMC using ANOVA and grey relational analysis," Int. J. Precis. Eng. Manuf., Vol. 12, No. 4, pp. 651-656, 2011.
11. Mandal, N., Doloi, B., and Mondal, B., "Force prediction model of Zirconia Toughened Alumina (ZTA) inserts in hard turning of AISI 4340 steel using response surface methodology," Int. J. Precis. Eng. Manuf., Vol. 13, No. 9, pp. 1589-1599, 2012.
12. Wyen, C. F. and Wegener, K., "Influence of cutting edge radius on cutting forces in machining titanium," CIRP Annals - Manuf. Technol., Vol. 59, pp. 93-96, 2010.